DEVELOPMENT OF BUCKET SCOOPING MECHANISM FOR ANALYSIS OF REACTION FORCE AGAINST ROCK PILES

Yuta TAKAHASHI, Ryohtaroh YASUHARA,
Osamu KANAI, Hisashi OSUMI
Chuo University
Dept. Prec.Mech., Chuo University
1-13-27, Kasuga, Bunkyo-ku, Tokyo 112-8551, Japan
yuta.1@arc2.mech.chuo-u.ac.jp

Shigeru SARATA
Intelligent Systems Institute, AIST
Namiki 1-2-1, Tsukuba, Ibaraki, 305-8564, JAPAN

Abstract: A bucket control mechanism is developed for the simulation of rock pile scooping by wheel loaders. By measuring the reaction forces from the scooped rock pile by a six axis force sensor installed into this mechanism, the reaction force model can be obtained and its parameters are identified. By using the obtained model for controlling actual wheel loaders, efficient scooping can be expected. In this paper, the kinematic and static characteristics of the bell-crank mechanism are analyzed and an experimental system is designed and built up using the analysis results. Then, a high gain servo control system is designed by using disturbance observers. The acquisition of the accurate rock pile model is tried by several experiments. Then some control algorithms based on feedback signals from the force sensor are proposed and their control performances are evaluated.

Keywords: wheel loader, autonomous scooping, rock pile, reaction force

1. Introduction

Automation of construction machines is strongly desired for various fields such as mining or disaster-relief works in addition to construction tasks[5][6]. A wheel loader is one of the most popular construction machines used in such sites. The automation of wheel loaders, however, is not achieved because of the difficulties of scooping tasks which need the rock pile model[8] applicable to the control algorithm. In order to build the control model of the rocks, theoretical analysis and its verification by using actual machines are essential. However, there are very few works for measuring actual reaction forces from rock piles during the bucket motion.

Therefore, in this paper, a miniature mechanical experimental system for the scooping is developed with the structure similar to a commercial wheel loader. By using the system, the reaction forces against rock piles can accurately be measured and it also helps the verification of the effectiveness of the designed scooping algorithms.

In Section 2, a reaction force model from a rock pile is divided into five components, and the relationship between the phase of scooping and the critical components in each phase is shown. In Section 3, the kinematics and statics of the developed mechanism is analyzed. Its effectiveness is verified by the results of fundamental experiments.

2. Reaction Force Model From Rock Pile

2.1 Component of reaction force from rock pile

The reaction force from a rock pile is divided into five components by Hemami[1][2]. Fig.1 shows the classification of the reaction forces. Each component shows the following force[3][4][7][9].

F_1: weight of rocks in the bucket
F_2:reaction force from rocks under the bucket
F_3:reaction force for inserting the bucket edge
F_4:friction force on the surface of the bucket
F_5: the reaction force from the anterosuperior soils moved by the bucket

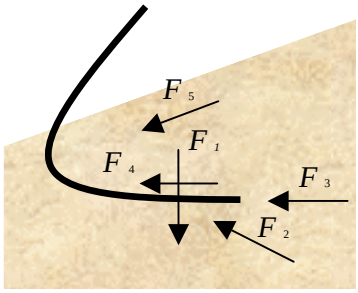

Fig.1 Five components of reaction force

2.2 Relationship between scooping phase and components of reaction force

The five components are not always acting on the bucket. According to the steps of scooping, forces acting on the bucket change.

(1) The former of insertion phase
At first, the rock pile does not move in spite of the insertion of the bucket. In this process the insertion resistance F_3 and friction forces F_4 are dominant. F_4 becomes the function of F_1 and F_5. In this phase F_5 is the force which supports the slope of the pile and is called active soil pressure. (Fig.2)

(2) The latter of insertion phase
When rocks are reaching the circular arc of the bucket, some rocks stop around the arc which play a roll of a wall. Then the bucket can not proceed any more unless the bucket moves the rocks in the pile. As a result, the value of F_5 becomes very large. F_5 in

this phase is called passive soil pressure. This phase continues until the reaction force becomes equal to or larger than the maximum driving force of the bucket. (Fig.3)

(3) The former part of the scooping phase

When the bucket precedes upper side, soil weight also appears. (Fig.4)

(4) The latter part of the scooping phase

Once the bucked is filled with rocks, the bucket moves upwards straightly. In this process, the weight of the rocks is dominant. (Fig.5)

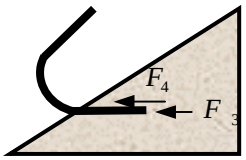

Fig.2 The beginning of penetrating step

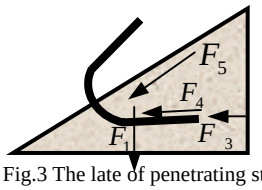

Fig.3 The late of penetrating step

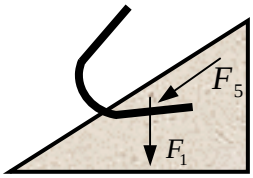

Fig.4 The beginning of scooping step

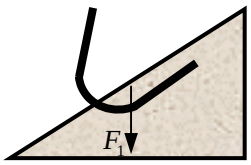

Fig.5 The late of scooping step

These theoretical values are formulated in the phase (1) and (2), and they were verified by fundamental experiments in the previous study[2]. On the other hand, those in the phase (3) and (4) are not formulated yet because of the lack of experimental data. Therefore they should be measured by experiments and formulated based on the experimental results.

Among these components, F_5 at the end of the phase (2) is supposed to be the largest value in the whole processes. It should be estimated before the design of the experimental system.

2.3 Passive Soil Pressure

The passive soil pressure F_5 is the force that moves the soil in front of the bucket so that the bucket goes forward. However, if the amount of the soil is too much, its value also becomes very large, and as a result, it becomes impossible for the bucket to proceed any more[3][4]. So it is essential to control a bucket avoiding increase of passive soil pressure. However it has not been made clear yet in what condition the passive soil pressure appears in scooping. By our previous research, the occurrence condition of passive soil pressure has assumed as follows.

Figure.6 shows the soil condition in the bucket. When the bucket inserts into the slope of soil, the soil flows into the bucket gradually. When the soil reaches the point of circular arc, its direction is changed and it goes along the arc. As a result, the angle between the soil pressure and the proceeding direction becomes large, and the soil stops soon. The soil staying around the position makes a fictitious face which is called virtual wall. It is expected that the passive soil pressure works without slip when the direction of the force gets in the friction corn as Fig.7.

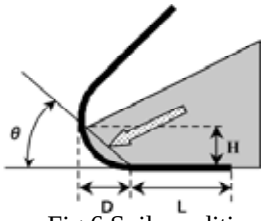

Fig.6 Soil condition

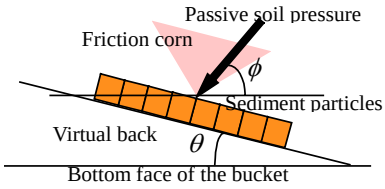

Fig.7 Passive soil pressure and friction

Therefore, a passive soil pressure decreases if the force direction gets out from the friction corn. In the other words, tilting motion of the bucket decreases a passive soil pressure. At the beginning of the phase (3), tilting motion is started. The largest value of F_5 in the end of the phase (2) will be estimated to design the mechanism in the following section.

3 Mechanism of Developed Experimental System

3.1 The outline of the developed mechanism

The developed mechanism is mechanistically equivalent to a real wheel loader. The size of the bucket is 100×100×250[mm] which is about 1/10 of the real loader. This mechanism consists of a 2 d.o.f. bucket driving mechanism and a moving table in a horizontal direction. The power transmission system to move the bucket in the former mechanism is a bell-crank mechanism which is suitable for hydraulic actuators. In the developed system, ball screw mechanisms and DC servo motors are used instead of hydraulic actuators. The bucket driving mechanism is mounted on the moving table through a six axes force sensor. The moving table plays a roll of a wheel driving system and is also driven by a DC servo motor. A By using a ball screw mechanism, small torque of the rotational motor can be converted to a large linear force. Encoders are installed into all the DC servo motors to measure the joint angles. Fig.8 and Fig.9 show the overall view of the mechanics.

Fig.8 The view of the developed mechanism

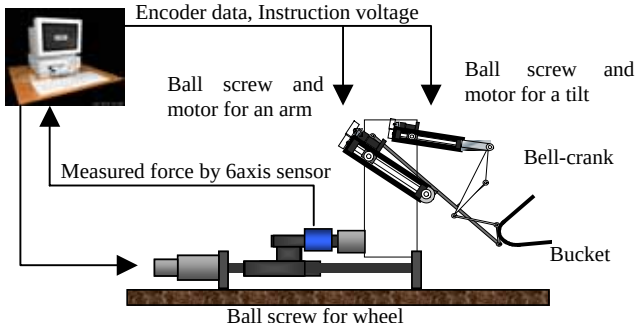

Fig.9 The organization of the developed mechanism

3.2 Kinematics of arm-bucket driving mechanism

The bucket is moved by the actuators through a bell-crank mechanism which is illustrated in Fig.10. The bucket is fixed to the bucket link GH, so the motion of the link GH corresponds to the bucket motion. The left end of the main arm OH is connected to a body mounted on the moving table through a passive rotational joint and rotates about O by the linear actuator 1. Triangle DEF is a link whose vertex E is connected to the part of the main arm OH through a passive joint. The bucket link GH is rotated by the linear actuator 2 through the link mechanism. As described above, both linear actuators consist of a ball screw mechanisms and the DC servo motors, and the other end of each linear actuator is also fixed to the same body in the same manner as the main arm.

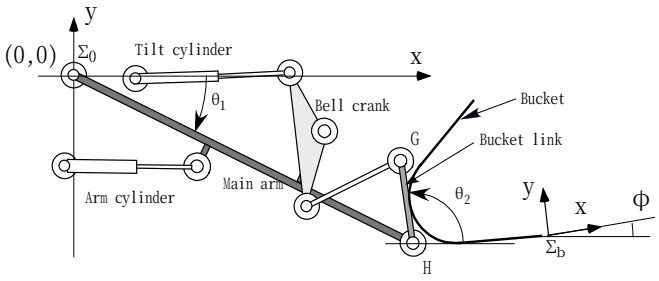

Fig.10 Bell-crank in the bucket driving mechanism

The reference frame Σ_o and the bucket coordinate Σ_b are defined as shown in Fig.10. The position and orientation of the bucket are also shown. Then, the relationship between the bucket position and orientation can be calculated as follows[7][10][11].

First, the angle of the main arm θ_1 and the length of the linear actuator l_1 is obtained. The angle α_1 is calculated by Eq. (1).

$$\alpha_1 = \cos^{-1}\left(\frac{{a_1}^2 + {d_1}^2 - {l_1}^2}{2a_1 d_1}\right) \qquad (1)$$

Then θ_1 is obtained as Eq. (2),

$$\theta_1 = \frac{\pi}{2} - (\alpha_1 - \delta_1) - \delta_2, \qquad (2)$$

where δ_1 is the angle shown in Fig.11 and it is determined by the kinematic parameters in advance.

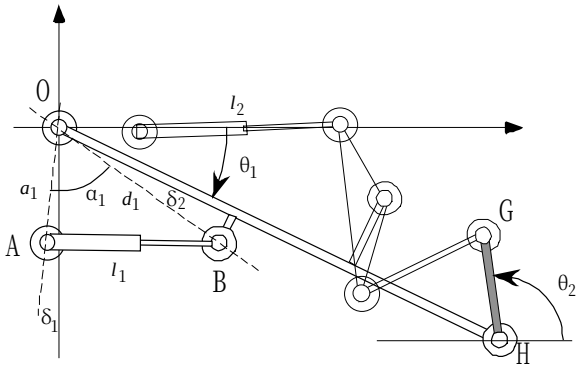

Fig.11 Kinematic parameters (1)

Next, the way to calculate the bucket position and orientation through the actuator lengths l_1 and l_2 is explained. Once the angle of the main arm OH θ_1 and that of the bucket link θ_2 shown in Fig.11 are determined, the bucket position and orientation are easily expressed by these two angles. Therefore, θ_2 is derived next. The coordinate of E is easily calculated by the kinematic parameters and θ_1 obtained as Eq.(2). Therefore, t_1 , the distance between C and E is calculated.

The angles ϕ_1 and ϕ_2 shown in Fig.12 are calculated by cosine theorem of triangle CDE. The shape of bell-crank is already known, so coordinates of point F can easily be calculated.

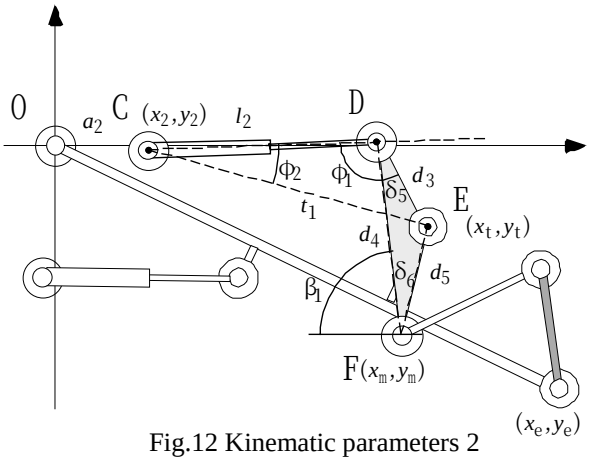

Fig.12 Kinematic parameters 2

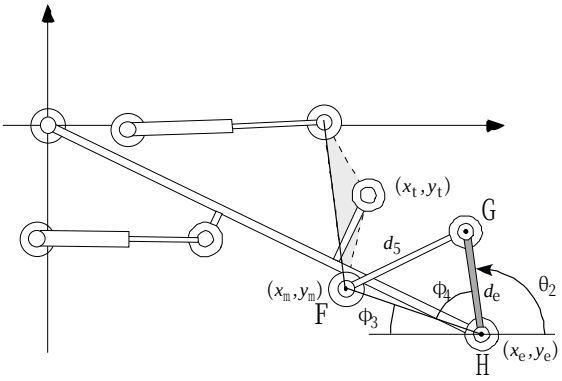

Fig.13 Kinematic parameters 3

The coordinate of point H can also be calculated by θ_1, so the angle of ϕ_4 is determined by applying the cosine theorem to the triangle FGH. The angle ϕ_3 is also calculated from coordinates of point F and H as Eq.(3) and Eq.(4).

$$\phi_3 = \tan^{-1}\frac{y_m - y_e}{x_e - x_m} \qquad (3)$$

$$\phi_4 = \cos\left(\frac{{d_e}^2 + {t_2}^2 - {d_6}^2}{2d_e t_2}\right) \qquad (4)$$

The angle of θ_2 is obtained through ϕ_3 and ϕ_4 as Eq.(5).

$$\theta_2 = \pi - \phi_3 - \phi_4 \tag{5}$$

3.3 Statics of the arm-bucket mechanism

Let the generated forces and moment at the origin of the bucket coordinate H be f_x, f_y and m as shown in Fig.14. Then, the forces required for the actuators f_{a1} and f_{a2} to generate f_x, f_y and m are calculated as follows.

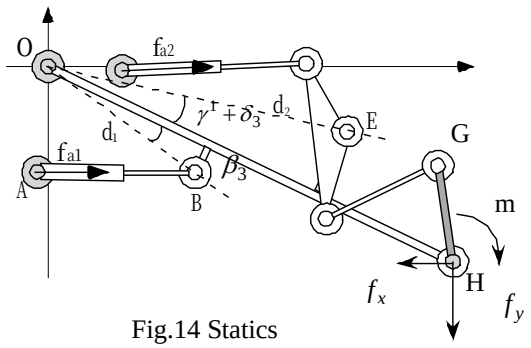

Fig.14 Statics

(1) calculation of f_{a2}

Figure 15 shows the applied forces and moments to the link GH. According to the moment equilibrium about H, the axial force of the link GH f_1 is determined as Eq.(6).

$$f_1 = \frac{m}{d_e \sin\phi_5} \tag{6}$$

According to the moment equilibrium about E, the actuator force f_{a2} is determined as the axial force expressed by Eq.(7),

$$f_{a2} = \frac{d_5 \sin\{\pi - (\theta_2 - \phi_5) - \beta_1 - \delta_6\}}{d_3 \sin(\pi - \phi_1)} f_1, \tag{7}$$

where parameters in Eq.(7) are shown in Fig.16.

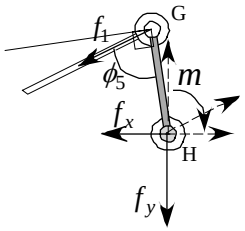

Fig.15 Forces and moment applied to link GH

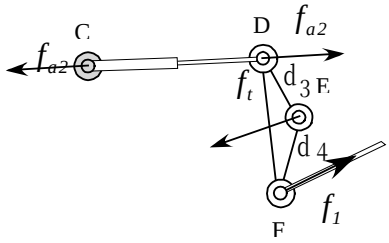

Fig.16 Forces and moments plied to bell-crank

(2) calculation of f_{a1}

The transmitted force $\mathbf{f}_t$ from the bell-crank to the main arm OH through the point E in Fig.14 is calculated as Eq.(8) from the force equilibrium on the bell-crank DEF.

$$\begin{aligned} f_{tx} &= f_1 \cos(\theta_2 - \phi_5) + f_{a2} \cos\{\pi - (\beta_1 + \phi_1 - \delta_5)\} \\ f_{ty} &= f_1 \sin(\theta_2 - \phi_5) + f_{a2} \sin\{\pi - (\beta_1 + \phi_1 - \delta_5)\} \end{aligned} \tag{8}$$

In addition, the applied force $\mathbf{f}_m$ from the link GH to the main arm OH through the point H is expressed as Eq.(9).

$$\begin{aligned} f_{mx} &= f_x + f_1 \cos(\theta_2 - \phi_5) \\ f_{my} &= f_y + f_1 \sin(\theta_2 - \phi_5) \end{aligned} \tag{9}$$

From Eq.(8) and Eq.(9), the moment about the point O due to the force $\mathbf{f}_t$ and $\mathbf{f}_m$ m_E and m_H are expressed as Eq.(10).

$$\begin{aligned} m_g &= f_{ty} d_2 \cos(\gamma_1 + \delta_3) + f_{tx} d_2 \sin(\gamma_1 + \delta_3) \\ m_d &= f_{my} L \cos(\theta_1) + f_{mx} L \sin(\theta_1) \end{aligned} \tag{10}$$

Then, the actuator force f_{a1} is obtained as Eq.(11) according to a moment equilibrium about the point O,

$$f_{a1} = \frac{m_d - m_g}{d_1 \sin(\beta_3)}, \tag{11}$$

where the angle β_3 is calculated as Eq.(12) from the cosine theorem of the triangle OAB.

$$\beta_3 = \cos^{-1} \frac{d_1^2 + l_1^2 - a_1^2}{2 d_1 l_1} \tag{12}$$

The actuators of the developed system should be chosen according to the calculation results of the above described statics. The DC motors were chosen under the assumption that the bucket lifts 25[kg] rocks at a time. Table 1 shows the specifications of actuators and the developed bucket driving mechanism. It can be seen that the required force for the cylinder AB is about 5 times larger than the output force.

Table 1 Specifications of the bucket driving system

Data	Arm cylinder	Tilt cylinder
Motor's nominal voltage	24[Volt]	42[Volt]
Using voltage	24[Volt]	24[Volt]
Motor's rotation frequency	10600[rpm]	7530[rpm]
Mortor's maximum torque	30.7[mNm]	113[mNm]
Gear ratio	1:4.8	1:4.8
Gear loss	×0.7	×0.7
Pitch of ball screw	2[mm]	1[mm]
Required force for cylinder(25kg)	1184[N]	447[N]
Maximum force of cylinder	1227.11[N]	583.31[N]
Maximum cylinder's velocity	27[mm/sec]	25[mm/sec]
Encorder resolution	2000[Pulse]	2000[Pulse]
Cylinder resolution	0.0002[mm]	0.0001[mm]
Bucket angle resolution	0.0002[deg]	0.0023[deg]

4 Experiment for measuring the reaction forces using the developed system

The experiments were performed to examine the effect of a bucket tilting motion on reaction forces from the rock pile.

The rocks used in the experiment are crushed rock of granite, and each size is about 4mmx4mmx4mm. Its specific gravity is about 2.7[g/cm^3]. The repose angle of this rock is about 40[deg]. And then, mountain of rock piles was 18 centimeters high and piled at a slope of repose angle.

In the experiment, the bucket is inserted into a rock pile horizontally until 22[s] and then bucket is lifted. When the bucket is lifted, two experimental conditions are examined. The first condition is that the bucket is lifted without tilt motions, and the other is with tilt motion from 22[s] to 23[s] at 2.7[deg/s].

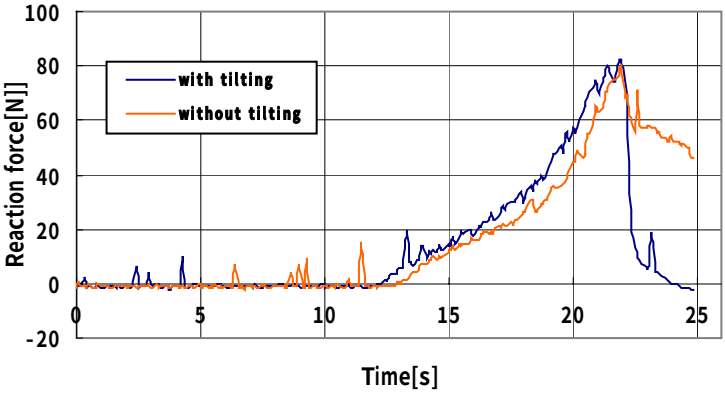

Fig.17 The change of the reaction force

The results are shown in Fig.17. This change of reaction force is very similar to it expected. The orange line indicates the reaction forces without tilting, and the blue line with tilting. According to the charts, both of the reaction forces start to increase from 13[s]. It shows that the insertion of the bucket into the rocks starts at the moment. The reaction forces become larger from 13[s] to 17[s] at the same rate. And then, increasing rates of reaction forces are grown up around 17[s]. This is attributed to the fact that passive soil pressure appears around 17 [s].

Both of forces were reduced at 22[s]. In the case without tilting motion, the arm couldn't scoop up the soils because the required output torque for the actuator to move the soils was larger than the maximum output torque.

On the other hand, the forces with tilting motion are drastically decreased in comparison with the forces without tilting. Therefore it is evident that the tilting motion of the bucket can be used to reduce reaction forces from soils.

5. Conclusions

The method of kinematics and static were calculated. According to this method, the new bucket-arm mechanism was developed. And then, the change of reaction force with tilting the bucket was revealed by experiments with the developed mechanism.

The formulation of each reaction forces should be defined with the data from new device as a next step. In addition, the occurrence condition of passive soil pressure should be revealed. Using this result, the new scooping algorithm will be suggested.

Reference

[1] A.Hemami; "Force analysis in the scooping/loading operation of an LHD Loader" , Proc. Of Mine Mechanization and Automation, Almgren, Kumar & vaganas(eds), pp415-424, 1993.

[2] A.Hemami; "Motion Trajectory Study in the Scooping Operation of an LHD-Loader", Transactions on INDUSTRY APPLICATIONS, vol.30, No.5, pp.1333-1338, 1994.

[3] H.Osumi, S.Sarata, Y.Hirai, O.Kanai: "Analysis of reaction force with a scooping soil", Proc. Symp. on Construction Robot, pp201-208, 2004.(in Japanese)

[4] Shigeru Sarata, Hisashi Osumi, Yoshihiro Kawai, Fumiaki Tomita; "Trajectory Arrangement based on Resistance Force and Shape of Pile at Scooping Motion", proc of the IEEE, ICRA, 2004.

[5] Sanjiv Singh, Howard Cannon :"Multi-Resolution Planning for Earthmoving", proc. of the IEEE, pp.121-126,ICRA, 1998.

[6] Sanjiv Singh, Reid Simmons: "Task Planning for Robotic Excavation", proc. of International Conference on Intelligent Robot Systems Raleigh", IROS, 1992.

[7] Y. H. Zweiri, L.D.Seneviratne, Kaspar Althoefer; "Prameter Estimation for Excavator Arm Using Generalized Newton Method", Transactions on ROBOTICS, Vol.20, No.4, pp.762-767, 2004.

[8] H.Takahashi et al; "Analysis on the Resistice Forces Acting on the Bucket of a Load-Haul-Dump Machine and a Wheel Loader in the Scooping Task", Advanced Robotics, Vol.13, No.2, pp.97-114, 1999.

[9] Choo Par Tan, Yahya H. Zweiri, Kaspar Althoefer, Lakmal D.Seneviratne, "Online Soil Parameter Estimation Scheme Based on Newton-Raphson Method for Autonomous Excavation", Trans. on MECHATRONICS, Vol.10, No.2, pp.221-229, 2005.

[10] Don Carter, Andrew Alleyne, Mechanical :"Load Modeling and Emulation for an Earthmoving Vehicle Powertrain", Proc. of the American Control Conference, pp.4963-4968, 2003.

[11] Roger Fales, Atul Kelkar, “Robust Control Design for a Wheel Loader Using Mixed Sensitivity H-infinity and Feedback Linearization Based Methods”, Proc. of American Control Conference, pp.4381-4386, 2005.